Engineering Structures 46 (2013) 38–48

Contents lists available at SciVerse ScienceDirect

Engineering Structures

journal homepage: www.elsevier.com/locate/engstruct

Application of evolutionary operation to the minimum cost design of continuous prestressed concrete bridge structure

Shohel Rana [a,*], Nazrul Islam [a], Raquib Ahsan [a], Sayeed Nurul Ghani [b]

[a] Department of Civil Engineering, Bangladesh University of Engineering and Technology (BUET), Dhaka-1000, Bangladesh
[b] Optimum System Designers, 2387 E Skipping Rock Way, Tucson, AZ 85737, USA

ARTICLE INFO

Article history:
Received 15 February 2011
Revised 11 July 2012
Accepted 17 July 2012
Available online 8 September 2012

Keywords:
Minimum cost design
Global optimization
Bridge structure
Prestressed concrete
Design variables
Constrained evolutionary operation

ABSTRACT

This paper implements an evolutionary operations based global optimization algorithm for the minimum cost design of a two span continuous prestressed concrete (PC) I-girder bridge structure. Continuity is achieved by applying additional deck slab reinforcement in negative flexure zone. The minimum cost design problem of the bridge is characterized by having a nonlinear constrained objective function, and a combination of continuous, discrete and integer design variables. A global optimization algorithm called EVolutionary OPeration (EVOP), is used which can efficiently solve the presented constrained minimization problem. Minimum cost design is achieved by determining the optimum values of 13 numbers of design variables. All the design constraints for optimization belong to AASHTO Standard Specifications. The paper concludes that the robust search capability of EVOP algorithm has efficiently solved the presented structural optimization problem with relatively small number of objective function evaluation. Minimum design achieved by application of this optimization approach to a practical design example leads to around 36% savings in cost.

1. Introduction

Most important criteria in structural design are serviceability, safety and economy. Structural engineers usually try to determine the optimum design that satisfies all performance requirements as well as minimize the cost of the structure. Advances in numerical optimization methods, computer based numerical tools for analysis and design of structures and availability of powerful computing hardware have all significantly aided the design process to ascertain the optimum design.

Many numerical optimization methods have been developed during last decades for solving linear and nonlinear optimization problems. Some of these methods are gradient based and search for a local optimum by moving in a direction related to the local gradient. Other methods apply first and second order necessary conditions to seek a local minimum by solving a set of nonlinear equations. For optimization of large engineering structures, these methods become inefficient due to large amount of associated gradient calculations and finite element analyses. Furthermore, when the objective function and constraints contain multiple or sharp peaks, the gradient based search becomes difficult and unstable. This difficulty has led to research on various new and innovative techniques which are found to be efficient and robust in solving complex and large structural optimization problems [1–11]. A constrained optimization algorithm EVolutionary OPeration (EVOP) [12], one of these new tools has been successfully applied for locating the global minimum [12–14]. It has been tested on a 10-variable objective function containing thousands of local minima [14] and has succeeded in locating the global minimum on completion of just the first pass. For 6-digit convergence accuracy it required only around 3000 objective function evaluations. Further, EVOP is capable of handling design vector containing mixed integer, discrete and continuous variables.

Optimization of bridge structures has not been attempted extensively as there are some complexities in formulating the optimization problem. These are presence of large number of design variables, discrete values of variables, discontinuous constraints and difficulties in formulation [15]. Adeli and Sarma [15] and Hassanain and Loov [16] have presented review of articles pertaining to cost minimization of prestressed concrete bridge structures. Some researchers [17–21] have used linear programming methods for minimum cost PC bridge design. Others [22–25] have used nonlinear programming techniques instead. Kirsch [26] used two level optimization of PC beam by using both linear and nonlinear programming technique. Genetic Algorithm has also been used by Ayvaz and Aydin [27] to minimize the cost of pre-tensioned PC I-girder bridges. Ahsan et al. [28] has recently demonstrated successful use of EVOP in cost optimum design of simply supported post-tensioned bridge.

The focus of this research is also on the evaluation of the effectiveness of the global optimization algorithm – EVOP developed by

* Corresponding author. Mobile: +880 1817011715.
E-mail addresses: shohel@ce.buet.ac.bd, shohel.ce@gmail.com (S. Rana).

0141-0296/$ - see front matter
http://dx.doi.org/10.1016/j.engstruct.2012.07.017

Ghani [12] in handling optimization problems of engineering structures particularly bridge structures. The bridge considered is a two span continuous post-tensioned PC I-girder structure. It is made continuous for superimposed dead loads and live loads by using negative flexural reinforcement in the deck slab. Large number of design variables and constraints are considered for cost minimization of the bridge system. A computer program is developed in C++ to formulate and execute the minimization problem.

2. Optimization algorithm – EVOP

In the present minimization problem, 13 numbers of design variables and a large numbers of constraints are associated. The design variables are categorized as continuous, discrete and integer types. The minimum cost design problem is subjected to highly nonlinear, implicit and discontinuous constraints that have multiple local minima requiring an optimization method that seeks the global optimum (Fig. 1). A global optimization algorithm, EVOP is used in this study. It has the capability to locate directly with high probability the global minimum within the first few automatic restarts. It also has the ability to minimize directly an objective function without requiring information on gradient or sub-gradient. There is no requirement for scaling of objective and constraining functions. It has facility to check whether the previously obtained minimum is the global minimum by user defined number of automatic restarts.

The algorithm can minimize an objective function

$$F(\underline{\boldsymbol{x}}) = F(x_1, x_2 \ldots x_N) \quad (1)$$

where $F(\underline{\boldsymbol{x}})$ is a function of n independent variables $\underline{\boldsymbol{x}} = (x_1, x_2, \ldots, x_N)$.

Explicit constraints (Eq. (2)) are imposed on each of the N independent variables x_i's ($i = 1,2,\ldots,N$).

$$ECL_i \leqslant x_i \leqslant ECU_i \quad (2)$$

where ECL_i's and ECU_i's are lower and upper limits on the variables respectively. They should be either constants or functions of N independent variables (moving boundaries). The explicit constraints are, however, not allowed to make the feasible vector-space non-convex.

Some implicit constraints (Eq. (3)) are also imposed on these n independent variables x_i's which are indirectly related to the design variables.

$$ICL_j \leqslant f_j(x_1, x_2 \ldots x_N) \leqslant ICU_j \quad (3)$$

where $j = 1,2,\ldots,m$. ICL_j's and ICU_j's are lower and upper limits on the m implicit constraints respectively. They can be constants or functions of the N independent design variables. The implicit constraints are allowed to make the feasible vector-space non-convex.

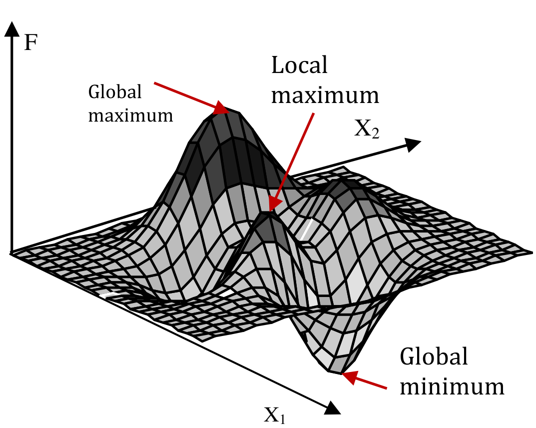

Fig. 1. Global and local optima of a 2-D function.

The algorithm is composed of six basic processes that are fully described in Ref. [12]. In this paper only a brief introduction to the algorithm is provided together with some illustrations. In order to understand the algorithm, at first it is necessary to know what a "complex" is. A 'complex' is an object that occupies an N-dimensional parameter space inside a feasible region defined by $K \geqslant (N+1)$ vertices inside a feasible region. where N is the number of independent design variables. It can rapidly change its shape and size for negotiating difficult terrain and has the intelligence to move towards a minimum. Fig. 2 shows a 'complex' with four vertices [12] in a two dimensional parameter space (X_1 and X_2 axes), where X_1 and X_2 are the two independent design variables. The 'complex' vertices are identified by lower case letters 'a', 'b', 'c' and 'd' in an ascending order of function values, i.e. $F(a) < F(b) < F(c) < F(d)$. Each of the vertices has two co-ordinates (X_1, X_2). Straight line parallel to the co-ordinate axes are explicit constraints with fixed upper and lower limits. The curved lines represent implicit constraints set to either upper or lower limits, and the hatched area is the two dimensional feasible region. A three dimensional representation of an objective function, $F = F(X_1, X_2)$ with two design variables (X_1, X_2) is shown in Fig. 3 which also represents a typical complex with four vertices 'a', 'b', 'c' and 'd' lying on the 2-dimensional parameter space (X_1X_2 plane).

The six basic processes of algorithm, EVOP are: (i) generation of a 'complex', (ii) selection of a 'complex' vertex for penalization, (iii) testing for collapse of a 'complex', (iv) dealing with a collapsed 'complex', (v) movement of a 'complex', and (vi) convergence tests [12]. These six processes are illustrated in Fig. 4.

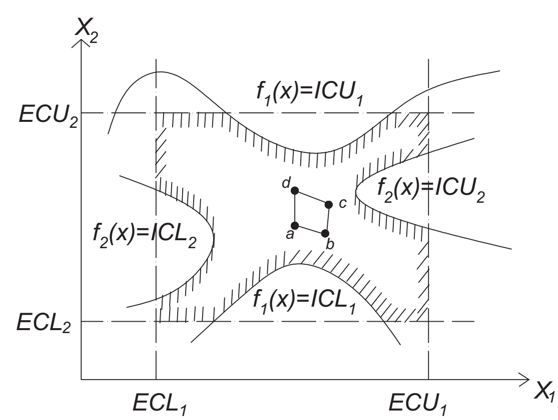

Fig. 2. A "complex" with four vertices [12].

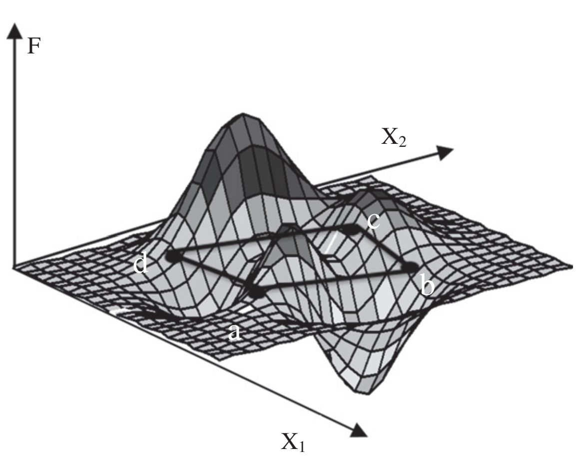

Fig. 3. A "complex" with four vertices in X_1X_2 plane.

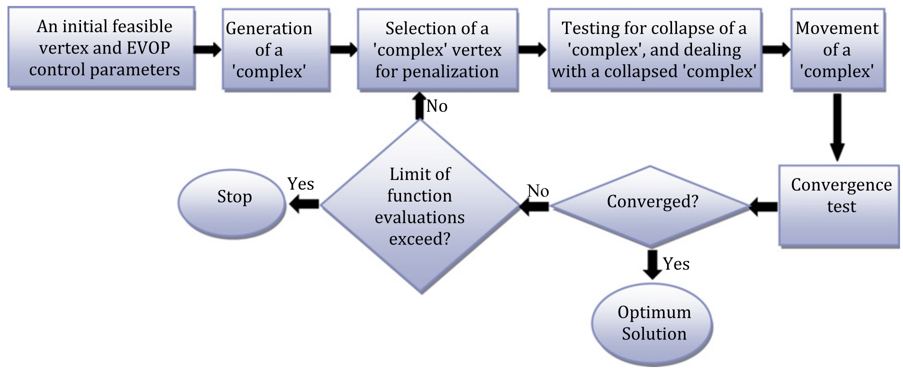

Fig. 4. Processes of EVOP algorithm.

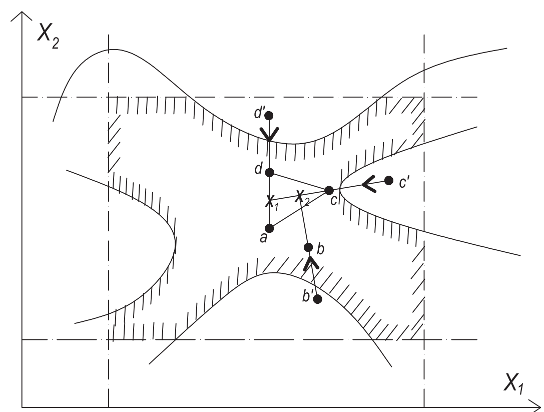

Fig. 5. Generation of initial "complex" [12].

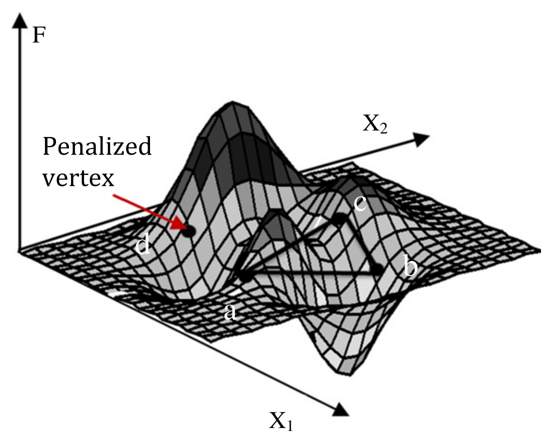

Fig. 6. Selection of a complex vertex for penalization.

2.1. Generation of a 'complex'

A 'complex' is generated beginning with a user provided starting point that satisfies all explicit and implicit constraint sets. Generating this feasible starting point is simple and described elsewhere [28]. Referring to Fig. 5, for any feasible parameter space a second point '*b*' is randomly generated within the bounds defined by the explicit constraints [12]. The coordinates of this random point is given by:

$$x_i \triangleq ECL_i + r_i(ECU_i - ECL_i) \quad \text{where } (i = 1, 2 \ldots N) \tag{4}$$

where r_i is a pseudo-random deviate of rectangular distribution over the interval (0,1).

If this second point also happens to satisfy all implicit constraints, then everything is going fine. The centroid of the two feasible points is next determined. If it satisfies all constraints, then things are really going fine and the 'complex' is updated with this second point. If, however, the randomly generated point fails to satisfy the implicit constraints it is continually moved half way towards the feasible starting point till all constraints are satisfied. Feasibility of the centroid of the two points is next checked. If the centroid satisfies all constraints, then we have an acceptable 'complex', and we proceed to generate the third feasible point for the 'complex'. If, however, the centroid fails to satisfy any of the constraints this second point is once again randomly generated in the space defined by the explicit constraints and the process repeated till a feasible centroid is obtained. Thus beginning from a single feasible starting point, all remaining $(k - 1)$ vertices of the 'complex' are generated that satisfy all explicit and all implicit constraints.

2.2. Selection of a 'complex' vertex for penalization

In this step, the worst vertex is penalized. The worst vertex of a 'complex' is that with the highest function value which is penalized by over-reflecting on the centroid (Fig. 6). For selection of a 'complex' vertex for penalization the procedure shown in Fig. 7 is followed until a preset number of calls to the three functions (implicit, explicit and objective) are collectively exceeded.

2.3. Testing for collapse of a 'complex'

A 'complex' is said to have collapsed in a subspace if the *i*th coordinate of the centroid is identical to the same of all '*k*' vertices of the 'complex' (Fig. 8). This is a sufficiency condition and detects collapse of a 'complex' when it lies parallel along a coordinate axis. Once a 'complex' has collapsed in a subspace it will never again be able to span the original *N*-dimensional space. The word "identical" here implies "identical within the resolution of Φ_{cpx} which is a parameter for detection of 'complex' collapse. Numbers *x* and *y* are considered to be identical within the resolution of Φ_{cpx} if *x* and $\{x + \Phi_{cpx}(x - y)\}$ have the same numerical values. For Φ_{cpx} set to 10^{-2}, if *x* and *y* differ by not more than the last two least significant digits they will be considered identical.

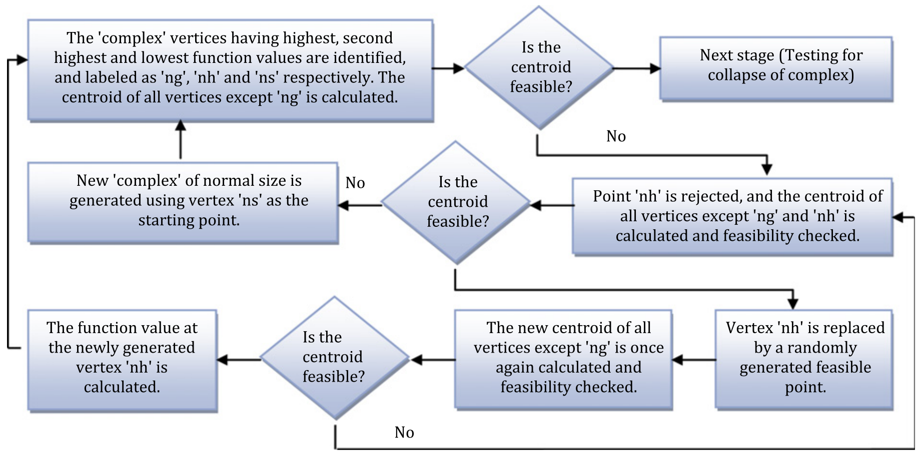

Fig. 7. Selection of a 'complex' vertex for penalization.

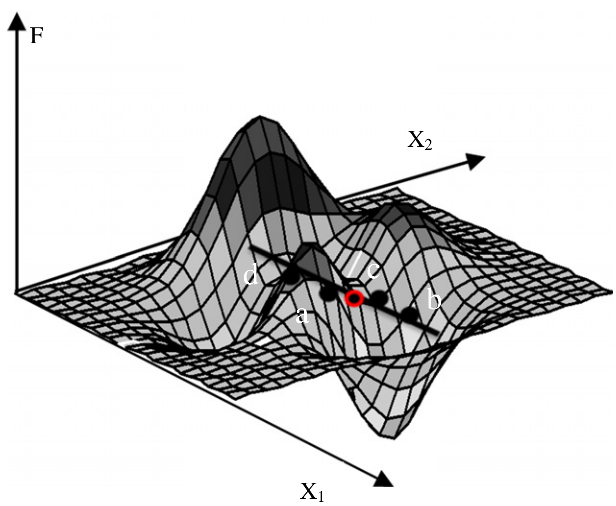

Fig. 8. Collapse of a 'complex.

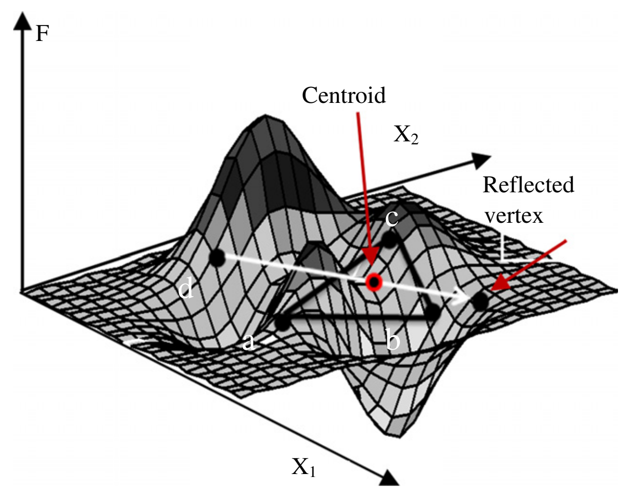

Fig. 9. Movement of a 'complex'.

2.4. Dealing with a collapsed 'complex'

After detecting the collapse of a 'complex' onto a subspace certain actions are taken such that a new full sized 'complex' is generated. It now fully spans the *N*-dimensional feasible space defined by the explicit and implicit constraints. The 'complex' is next moved as described below.

2.5. Movement of a 'complex'

In a nutshell the process begins by selecting the worst vertex '$ng = d$' of the current 'complex' '*abcd*' for penalization and then ascertaining feasibility of the centroid of the remaining $(k-1)$ vertices '*abc*'. If it is found to be infeasible, then appropriate steps are taken to regain its feasibility. The worst vertex '$ng = d$' is next penalized by over-reflecting (Fig. 9) it on the feasible centroid of the remaining vertices to generate a new feasible trial point x_r,

$$x_r = (1+\alpha)C - \alpha x_g \tag{5}$$

where α is reflection coefficient.

Outcome of this reflection step is next ascertained, and if found to be over successful then expansion step is executed using expansion coefficient (γ). If, however, the refection step is found to be unsuccessful, then either one of two types of contraction steps is applied both of which uses contraction coefficient (β). Application of expansion step or contraction step will generate a new feasible trial point, x_r. A full detail of this crucial step is fully described in a monograph [12].

2.6. Convergence tests

While executing the process, movement of a 'complex', tests for convergence are made periodically after certain preset number of calls to the objective function. There are two levels of convergence tests. The first convergence test would succeed only if a predefined number of consecutive lowest function values are identical within the resolution of the convergence parameter Φ, which should be greater (smaller value of negative exponent) then Φ_{cpx}. The second convergence test is attempted only if the above first convergence test succeeds. This second test verifies whether the function values at all vertices of the current 'complex' are also identical within the resolution of Φ.

3. Minimum cost design problem statement

Formulation and integration of the cost minimization problem for the bridge system to the optimization algorithm is shown in Fig. 10.

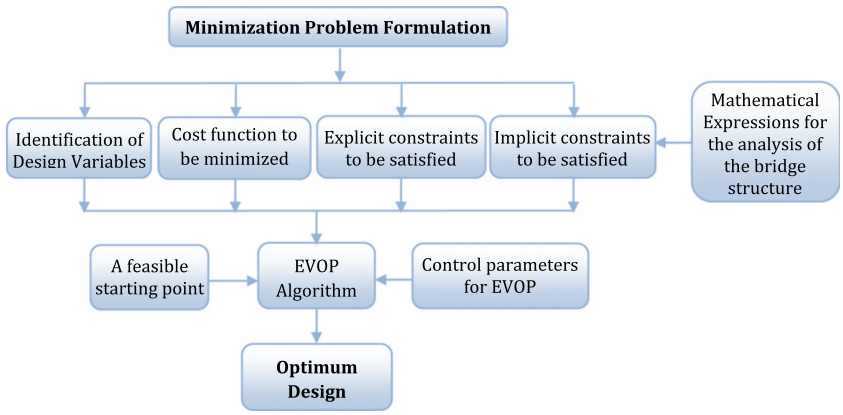

Fig. 10. Minimization problem formulation and linking with EVOP.

3.1. Design variables

For the minimum cost design of the presented two span continuous PC I-girder bridge structure (Fig. 11), the design variables considered are girder spacing, various cross sectional dimensions of the girder, number of strands per tendon, number of tendons, tendon layout and configuration, slab thickness, slab reinforcement and negative flexural reinforcement in the deck slab over pier. These variables are specifically mentioned in Table 1 and shown in Fig. 12. They are classified in three types as continuous, discrete and integer. To vary the tendon profile and arrangement, two design variables (lowest tendon position at the end section, y_1 and number of tendons at lowest layer of mid section, N_{TLM}) are considered as shown in Fig. 13. The vertical positions of other tendons are calculated according to the requirements of end bearing and anchorage system. Negative moment reinforcement is provided within the cast-in-place deck slab for live load continuity at interior supports.

3.2. Cost function

The total cost (C_T) of the bridge system consists of four components – C_{GC}, C_{DC}, C_{PS} and C_{OS}. Where C_{GC}, C_{DC}, C_{PS} and C_{OS} are the cost of materials, fabrication and installation of girder concrete, deck slab concrete, prestressing steel and ordinary steel for deck reinforcement, girder's shear reinforcement and reinforcement at negative moment section respectively. Hence, the total cost is formulated as:

$$C_T = C_{GC} + C_{DC} + C_{PS} + C_{OS} \quad (6)$$

Costs of individual components per girder are calculated as per the following equations:

$$C_{GC} = (UP_{GC}V_{GC} + UP_{GF}SA_G) \quad (7)$$

$$C_{DC} = (UP_{DC}V_{DC} + UP_{DF}SA_D) \quad (8)$$

$$C_{PS} = (UP_{PS}W_{PS} + 2UP_{ANC}N_{ANC} + UP_{SH}TL_{SH}) \quad (9)$$

$$C_{OS} = UP_{OS}(W_{OSD} + W_{OSG} + W_{OSN}) \quad (10)$$

where UP_{GC}, UP_{DC}, UP_{PS} and UP_{OS} are the unit prices including materials, labor, fabrication and installation of the precast girder concrete, deck concrete, prestressing steel and ordinary steel respectively. UP_{GF}, UP_{DF}, UP_{ANC}, UP_{SH} are the unit prices of girder formwork, deck formwork, anchorage set and metal sheath for duct respectively; V_{GC}, V_{DC}, W_{PS}, W_{OSD} and W_{OSG} are the volume of the precast girder concrete and deck slab concrete, weight of prestressing steel and ordinary steel in deck and in girder respectively; W_{OSN}

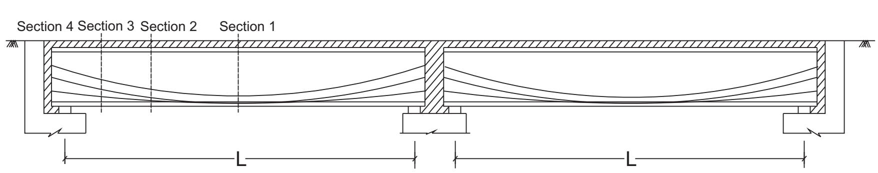

Fig. 11. Two span continuous post-tensioned I-girder bridge.

Table 1
Design variables.

Design variables	Variable name	Variable symbol	Variable type
Girder spacing (m)	X_1	S	Discrete
Girder depth (mm)	X_2	G_d	Discrete
Top flange width (mm)	X_3	TF_w	Discrete
Bottom flange width (mm)	X_4	BF_w	Discrete
Bottom flange thickness (mm)	X_5	BF_t	Discrete
Number of strands per tendon	X_6	N_s	Integer
Number of tendons per girder	X_7	N_T	Integer
Lowest tendon position at the end section (mm)	X_8	y_1	Continuous
Number of tendons at lowest layer of mid section	X_9	N_{TLM}	Integer
Initial stage prestress (% of full prestress)	X_{10}	η	Continuous
Slab thickness (mm)	X_{11}	t	Discrete
Slab main reinforcement ratio	X_{12}	ρ	Continuous
Reinforcement ratio in negative moment section	X_{13}	ρ_n	Continuous

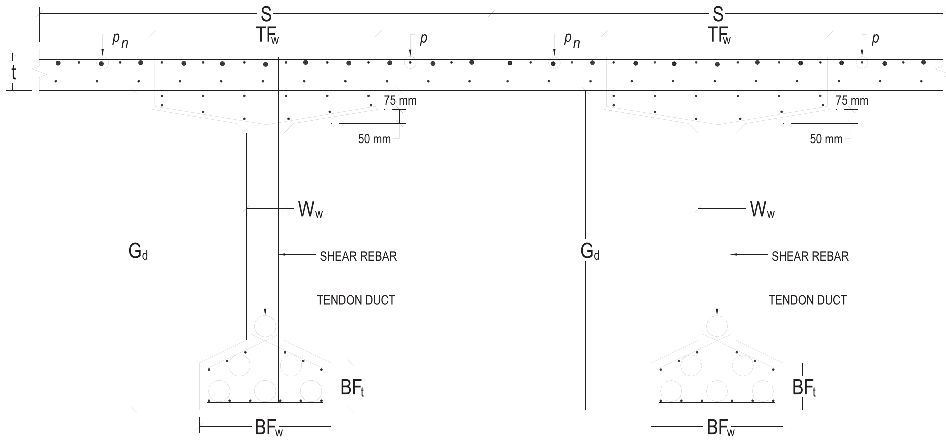

Fig. 12. Girder section with design variables.

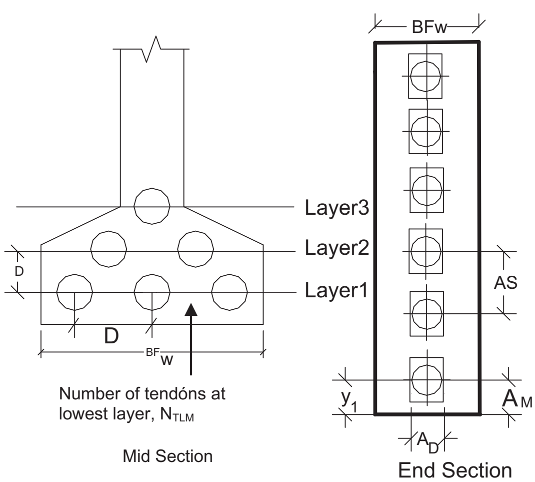

Fig. 13. Tendons arrangement in the girder.

is the ordinary reinforcement at negative moment section; SA_G and SA_D are the surface areas of the girder and the deck respectively; N_{ANC} is number of anchorages; TL_{SH} is total length of the tendon sheath.

3.3. Explicit constraints

These constraints are directly related to the design variables and restrict their range. They are specified limitations (upper or lower bounds) on design variables and are derived from various considerations such as functionality, fabrication, or aesthetics. A typical constraint is defined as:

$$X_L \leqslant X \leqslant X_U \tag{11}$$

where X = design variable, X_L = lower limit of the design variable, X_U = upper limit of the design variable. The explicit constraints for each of the design variables are shown in Table 2.

3.4. Implicit constraints

These constraints are indirectly related to the design variables and represent the performance requirements of the bridge system as per various specifications. A total of 51 implicit constraints are considered according to the AASHTO Standard Specifications (AASHTO) [29] and are classified into nine categories (IC-1–IC-9).

3.4.1. IC-1 (ultimate flexural strength constraints)

The ultimate bending moment capacities to carry all the required dead and live loads are considered both at maximum positive moment and negative moment sections. The ultimate flexural strength constraint is:

$$0 \leqslant M_u \leqslant \varphi M_n \tag{12}$$

where M_u is the factored bending moment and φM_n is the flexural strength of the girder.

3.4.2. IC-2 (ductility constraints)

According to AASHTO, two constraints are applied to limit the maximum and minimum values of the prestressing steel so that it yields when the ultimate capacity is reached (Eqs. (13) and (14)).

$$0 \leqslant w \leqslant w_u \tag{13}$$

$$1.2M^*_{cr} \leqslant \varphi M_n \tag{14}$$

where w = reinforcement index and w_u = upper limit to reinforcement index; M^*_{cr} = cracking moment of the girder.

Table 2
Explicit constraints.

Variable name	Variable symbol	Explicit constraint	Variable name	Variable symbol	Explicit constraint
X_1	S	$B_W/10 \leqslant S \leqslant B_W$	X_8	y_1	$A_M \leqslant y_1 \leqslant 1000$
X_2	G_d	$1000 \leqslant G_d \leqslant 3500$	X_9	N_{TLM}	$1 \leqslant N_{TLM} \leqslant N_T$
X_3	TF_w	$300 \leqslant TF_w \leqslant S$	X_{10}	η	$1\% \leqslant \eta \leqslant 100\%$
X_4	BF_w	$300 \leqslant BF_w \leqslant S$	X_{11}	t	$175 \leqslant t \leqslant 300$
X_5	BF_t	$a \leqslant BF_t \leqslant 600$	X_{12}	ρ	$\rho_{\min} \leqslant \rho \leqslant \rho_{\max}$
X_6	N_s	$1 \leqslant N_s \leqslant 27$	X_{13}	ρ_n	$\rho_{n\min} \leqslant \rho_n \leqslant \rho_{n\min}$
X_7	N_T	$1 \leqslant N_T \leqslant 20$			

Note: B_W = bridge width; a = clear cover + duct diameter; web width, W_w = clear cover + web rebars diameter + duct diameter; A_M = minimum vertical edge distance for anchorage; and $\rho_{\min}$ and $\rho_{\max}$ are respectively minimum and maximum permissible reinforcement of slab according to AASHTO (2002); $\rho_{n\min}$ and $\rho_{n\max}$ are respectively minimum and maximum permissible reinforcement at negative moment section.

3.4.3. IC-3 (flexural working stress constraints)

These constraints ensure stress in concrete not to exceed the allowable stress value both at transfer and under service loads. The constraints are given by:

$$\sigma^L \leqslant \sigma \leqslant \sigma^U \quad (15)$$

where

$$\sigma = -\frac{F}{A} \pm \frac{Fe}{S} \pm \frac{M}{S} \quad (16)$$

σ^L = allowable compressive stress (lower limit), σ^U = allowable tensile stress (upper limit) and σ_j = the actual working stress in concrete; A = cross sectional area of the girder; F, e, S, M = prestressing force, tendons eccentricity, section modulus and working moment respectively. These constraints are considered as per AASHTO at all the critical sections along the entire span of the girder as shown in Fig. 14, and for various loading stages (initial stage and service conditions). As prestress losses are also implicit functions of some of design variables, they are estimated according to AASHTO, instead of using lump sum value for greater accuracy.

3.4.4. IC-4 (ultimate shear strength and horizontal shear strength constraints)

The ultimate shear constraint (Eq. (17)) is satisfied to be less than or equal to the nominal shear strength times the resistance factor.

$$\varphi V_s \leqslant 0.67\sqrt{f_c'}W_w d_s \quad (17)$$

where V_s = shear carried by the steel in kN; W_w = width of web of the girder; d_s = effective depth for shear; and φ = strength reduction factor for shear.

Cast-in-place concrete decks designed to act compositely with precast girder must be able to resist the horizontal shearing forces at the interface between the two elements. The constraint for horizontal shear is,

$$V_u \leqslant \varphi V_{nh} \quad (18)$$

V_u = factored shear force acting on the interface; and V_{nh} = nominal shear capacity of the interface.

3.4.5. IC-5 (deflection constraint)

According to AASHTO Standard Specification PC girder having continuous spans is designed so that the deflection due to service live load plus impact shall not exceed 1/800 of the span. Deflection constraint due to live load [30] is,

$$\Delta_{LL} = \frac{5L^2}{48E_cI_c}[M_{\max} - 0.1(M_a + M_b)] \leqslant \frac{L}{800} \quad (19)$$

where $M_{\max}$ = the maximum positive moment due to live load; M_a and M_b = the corresponding negative moment at the ends of the span being considered; E_c = modulus of elasticity of girder concrete and I_c = moment of inertia of the composite girder section.

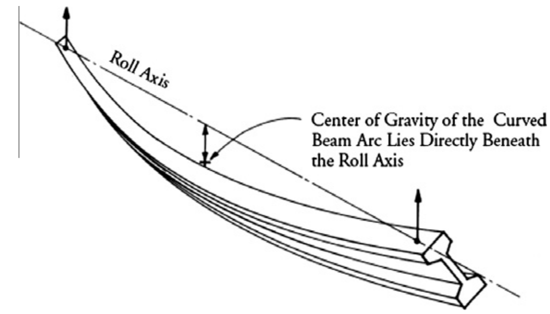

Fig. 15. Perspective of a girder free to roll and deflect laterally [31].

3.4.6. IC-6 (tendon profile constraint)

This constraint limits the tendon profile so that the extreme fiber tension remains within the allowable limits. It is,

$$\frac{G_d}{6} + 0.25\sqrt{f_{ci}'}\frac{A_EG_d}{6F_i} \leqslant e \leqslant \frac{G_d}{6} + 0.5\sqrt{f_c'}\frac{A_EG_d}{6F_e} \quad (20)$$

where A_E = cross-sectional area of the end section of the girder; F_i, F_e are prestressing forces after instantaneous losses and all losses at end section respectively; and f_{ci}', f_c' = initial and 28 days compressive strengths of girder concrete respectively.

3.4.7. IC-8 (deck slab constraint)

For ultimate strength design of deck slab, the constraint related to required effective depth for deck slab is,

$$D_{\min} \leqslant d_{req} \leqslant d_{prov} \quad (21)$$

where d_{req}, d_{prov}, $d_{\min}$ = required, provided and minimum effective depth of deck slab respectively.

3.4.8. IC-9 (lateral stability constraint)

During handling and transportation, support conditions may result in lateral displacements of the beam, thus producing lateral bending about the weak axis (Fig. 15). The following constraint, according to PCI [31], ensures the safety and stability during lifting of long girder subject to roll about the weak axis,

$$FS_C \geqslant 1.5 \quad (22)$$

where FS_c = factor of safety against cracking of top flange when the girder hangs from the lifting loop.

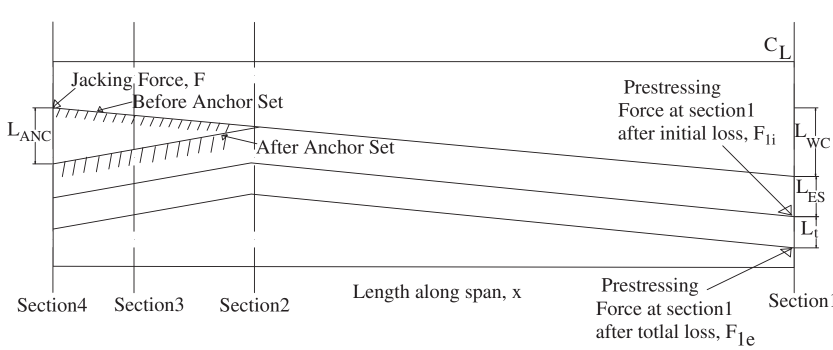

Fig. 14. Variation of prestressing force along the length of girder.

4. Practical example and discussion

In this section, an example is provided to demonstrate the application of the optimization approach presented in this paper. The example consists of two span continuous post-tensioned PC I-girder bridge structure (each span = 50 m) made composite with cast-in situ deck slab. Continuity is achieved by applying mild steel reinforcement in the deck slab. The girder is made continuous for live load and superimposed dead loads only. The constant design parameters used are summarized in Tables 3 and 4. The relative cost data for materials, labor, fabrication and installation used are obtained from the Roads and Highway Department (RHD) cost schedule [32].

The EVOP code is written in FORTRAN. A computer program coded in the C++ language is used to analyze the bridge structure, to input the control parameters, to code the objective function, the function to evaluate explicit constraints and the function to evaluate implicit constraints and to define a starting point inside the feasible space. The program is then integrated with EVOP using the technique of FORTRAN to C++ conversion.

To begin with, the values of the control parameters are assigned with their default values and other input parameters are set to specific numerical values as tabulated in Tables 5 and 6. The EVOP control parameters α, β, γ are next varied sequentially within the recommended range for successful convergence and lowest number of objective function evaluation. The most sensitive parameter is α. Numerical values of the parameters Φ and Φ_{cpx} are then gradually increased in decade steps, making sure Φ is a decade or two greater than Φ_{cpx}. The above process is repeated to obtain greater convergence accuracy. NRSTRT is the number of automatic restart of EVOP to check that the previously obtained value is the global minimum. If NRSTRT = 50, the EVOP program will execute 50 times. For first time execution a starting point of the complex inside the feasible space has to be given. For further restart the complex is generated taking the coordinates of the previous minimum (values obtained from previous execution of EVOP) as the starting point of the complex.

Table 3
Bridge design data and material properties.

Bridge design data	Material properties
Two span continuous (each span = 50 m)	Ultimate strength of prestressing steel, f_{pu} = 1861 MPa
Girder length = 50 m (L = 48.8 m)	Yield stress of ordinary steel, f_y = 410 MPa
Bridge width, B_W = 12.0 m (three lane)	Girder concrete strength, f'_c = 50 MPa
Live load = HS20–44	Deck slab concrete strength, f'_{cd} = 25 MPa
No. of diaphragm = 4; diaphragm width = 250 mm	Initial girder concrete strength, f'_{ci} = 30 MPa
Wearing surface = 50 mm	Wobble and friction coefficients, K = 0.005/m
Curb height = 600 mm; curb width = 450 mm	Friction coefficients, μ = 0.25
7 Wire 15.2 mm diameter low-relaxation strand	Anchorage slip, δ = 6 mm
Freyssinet anchorage system [33]	

Table 5
Control parameters for EVOP.

EVOP control parameters	Default values	Range
Reflection coefficient, α	1.2	1.0–2.0
Contraction coefficient, β	0.5	0–1.0
Expansion coefficient, γ	2.0	>1.0
Convergence parameter, Φ	10^{-13}	10^{-16}–10^{-8}
Parameter to detect collapse of complex, Φ_{cpx}	10^{-14}	10^{-16}–10^{-8}
Explicit constraint retention coefficient, Δ	10^{-12}	

Table 6
Input parameters for EVOP.

Input parameters with values
Number of complex vertices, K = 14
Maximum number of times the three functions can be collectively called, LIMIT = 100,000
Dimension of the design variable space, N = 13
Number of implicit constraint, NIC = 51
Number of EVOP restart, NRSTRT = 50

4.1. Initial complex configuration

As there are 13 (N = 13) numbers of design variables in the proposed optimization problem, the complex will occupy a 13-dimensional parameter space having 14 ($K \geqslant N + 1$) number of vertices inside the feasible region. Each of the vertices will have 13 numbers of co-ordinates (X_1 to X_{13}) as shown in Table 7. After providing a feasible starting point (vertex no. 1 shown in Table 7), EVOP generates the remaining 13 vertices of the initial complex. Each vertex of the initial complex as shown in Table 7 is feasible solution or design of the bridge. It indicates that many alternative designs of the bridge can exist with different costs of the bridge. The cost of the bridge as shown in Table 7 typically varies from 81,718 US$ to 123,445 US$.

After first execution of EVOP, the coordinates for the minimum cost design are as shown in Table 8.

4.2. Restart of EVOP to check the minimum

Automatic restart of EVOP takes place to check whether the previously obtained minimum is the global minimum. The new initial

Table 4
Cost data.

Item	Unit	Total cost ($)	Material cost ($)	Labor cost ($)	Installation and fabrication cost ($)
Precast girder concrete-including equipment and labor (UP_{GC})	per m^3 (40 MPa)	180	60	45	75
Girder formwork (UP_{GF})	per m^2	5			5
Cast-in-place deck concrete (UP_{DC})	per m^3	85	68	13	4
Deck formwork-equipment and labor (UP_{DF})	per m^2	4.5			4.5
Girder posttensioning-tendon, equipment and labor (UP_{PS})	per ton	1285	1202	72	11
Anchorage set (UP_{ANC})	per set	65	65		
Metal sheath for duct (UP_{SH})	per lin. meter	1.3	1.3		
Mild steel reinforcement for deck and web in girder (UP_{OS})	per ton	640	595	44	1

Table 7
Vertices of initial complex.

Vertex no.	X_1 S (m)	X_2 G_d (mm)	X_3 TF_w (mm)	X_4 BF_w (mm)	X_5 BF_t (mm)	X_6 N_S	X_7 N_T	X_8 y_1 (mm)	X_9 N_{TLM}	X_{10} η (%)	X_{11} t (mm)	X_{12} ρ (%)	X_{13} ρ_n (%)	C_T (US$)
1	3.0	3000	1245	1200	255	10	7	930	7	53	210	0.628	0.300	99,105
2	3.0	2950	1225	1200	270	10	7	985	7	52	215	0.644	0.412	101,744
3	2.4	2975	1225	1200	260	10	7	960	7	53	210	0.627	0.336	119,498
4	3.0	2950	1325	1100	275	9	8	995	8	55	210	0.696	0.586	102,122
5	3.0	2875	1200	1175	300	9	8	890	7	52	215	0.802	0.486	103,907
6	3.0	2975	1250	1175	270	9	7	940	7	53	215	0.680	0.410	98,328
7	2.4	2775	1150	1150	320	8	8	1155	6	63	225	0.982	0.532	123,445
8	3.0	2925	1200	1125	305	10	8	1040	7	52	220	0.781	0.562	107,560
9	3.0	2900	1200	1200	280	9	7	1010	7	54	220	0.702	0.564	101,665
10	3.0	2925	1300	1350	260	11	8	1125	8	50	220	0.907	0.960	121,378
11	3.0	2875	1200	1225	285	9	8	990	7	52	220	0.80	0.568	106,576
12	3.0	2900	1225	1150	295	10	7	1025	7	55	215	0.810	0.511	103,542
13	3.0	2900	1200	1275	290	10	7	1100	7	60	215	0.80	0.525	107,015
14	3.0	2775	1425	600	295	10	6	738	3	54	230	0.61	0.683	81,718

Table 8
Value of design variables after first execution.

S (m)	G_d (mm)	TF_w (mm)	BF_w (mm)	BFt (mm)	N_S	N_T	y_1 (mm)	N_{TLM}	t (mm)	ρ (%)	ρ_n (%)	η (%)	C_T (US$)
3.0	2725	1500	525	200	7	5	967	4	210	0.60	0.63	46	67,239

Table 9
Value of design variables after restarts.

	S (m)	G_d (mm)	TF_w (mm)	BF_w (mm)	BF_t (mm)	N_S	N_T	y_1 (mm)	N_{TLM}	η (%)	t (mm)	ρ (%)	ρ_n (%)	C_T (US$)
First restart	3.0	2725	1500	525	200	7	5	965	4	46	210	0.60	0.62	67,179
Second restart	3.0	2800	1450	450	185	7	5	970	4	44	210	0.60	0.701	66,375
Third restart	3.0	2800	1450	450	185	7	5	970	4	44	210	0.60	0.698	66,366
Fourth restart	3.0	2600	1250	475	145	8	5	860	4	41	210	0.63	0.763	65,986

Table 10
Computational effort by EVOP.

	OF[a]	EC[a]	IC[a]	T (s)
First execution	463	2813	1621	10
First restart	170	3388	1719	
Second restart	424	9632	4813	
Third restart	36	319	200	
Fourth restart	79	504	336	

[a] Number of evaluations; OF = objective function; EC = explicit constraint; IC = implicit constraint; T = total time required for 50 restarts (s).

complex is generated taking the coordinates of the previous minimum (values obtained from previous execution of EVOP) as the starting point of the new complex. After four restarts of EVOP the coordinates for the minimum cost design are as shown in Table 9.

Further many restarts of EVOP give the same coordinates of the minimum as obtained after the fourth restart; that is no further improvement in the design could be obtained. It was, therefore, inferred that the coordinates of the minimum obtained after the fourth restart are indeed the optimum solutions, with a minimum objective function value of F = 65,986 US$. The computational

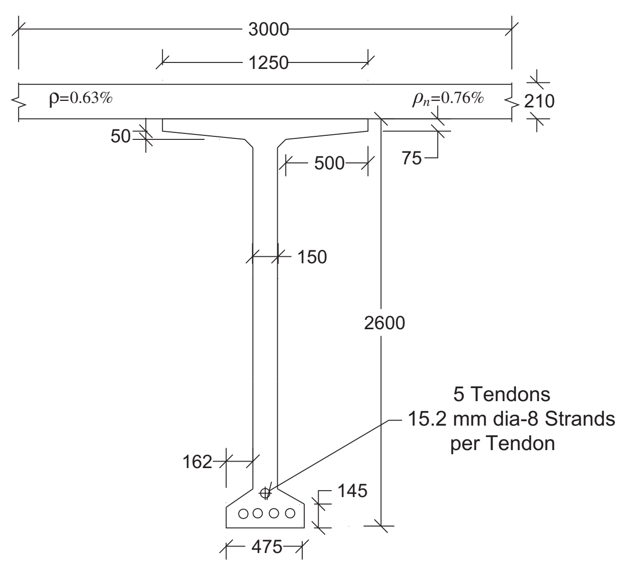

Fig. 16. Optimum values of design variables (dimensions are in mm).

Table 11
Minimum cost design and existing design.

	S (m)	G_d (mm)	TF_w (mm)	BF_w (mm)	BF_t (mm)	N_S	N_T	y_1 (mm)	N_{TLM}	t (mm)	ρ (%)	ρ_n (%)	η (%)	C_T (US$)
Minimum design	3.0	2600	1250	475	145	8 (0.6″ dia.)	5	860	4	210	0.63	0.76	53	65,986
Existing design	2.4	2500	1060	710	200	12 (0.5″ dia.)	7	400	4	188	0.82	–	43	102,480
Saving $= \frac{102{,}480-65{,}986}{102{,}480} \times 100 = 35.6\%$														

efforts by EVOP are tabulated in Table 10. The values of control parameters used are, $\alpha = 1.5$, $\beta = 0.5$, $\gamma = 2$, $\Phi = 10^{-13}$, $\Phi_{cpx} = 10^{-15}$.

The minimum cost design when compared with an existing conventional design of a PC I-girder bridge of same span [34] shows around 36% savings in cost. Table 11 compares the existing design and optimum design and their costs. Cross-sections showing the optimum design and the existing design are shown in Figs. 16 and 17.

Tendon profiles along the girder span are shown in Fig. 18 and Table 12. The optimization problem with 13 mixed type design variables and 51 implicit constraints converges with relatively small number of objective function evaluations (Table 10) with three digit convergence accuracy in the present problem of five digit objective functional value. The corresponding numbers of explicit and implicit constraints evaluations are also comparatively smaller. Intel COREi3 processor has been used in this study and computational time required for optimization by EVOP for 50 times restart, is around only 10 s.

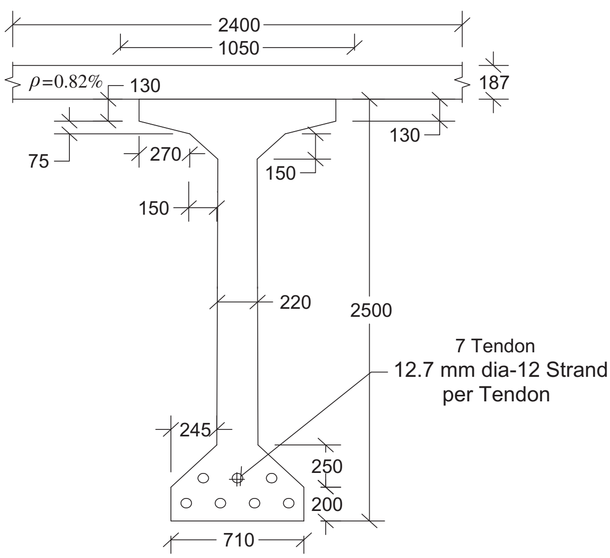

Fig. 17. Existing values of design variables (dimensions are in mm).

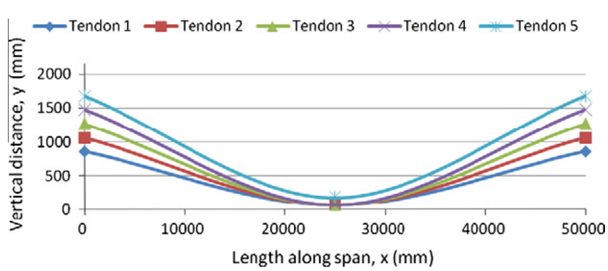

Fig. 18. Tendon profile in the minimum cost design.

Table 12
Tendon profile along the girder span.

x (mm)	Tendon 1 y (mm)	Tendon 2 y (mm)	Tendon 3 y (mm)	Tendon 4 y (mm)	Tendon 5 y (mm)
0	860	1065	1270	1475	1680
25000	73	73	73	73	181
50000	860	1065	1270	1475	1680

Table A1
Functional value of $f(X_6)$.

X_6	1–3	4	5–7	8–9	10–13	14–19	21–22	23–27
$f(X_6)$	125	130	145	150	165	180	190	195

5. Conclusions

In this paper, an optimization problem namely cost minimization of two-span continuous PC girder bridge is solved for a significant number of design variables pertaining to both the girders and the deck. A constrained global optimization algorithm named EVolutionary OPeration (EVOP) is used which is capable of locating directly with high probability the global minimum of an objective function of several variables and of arbitrary complexity subject to explicit and implicit constraints. A computer program in C++ is developed for the minimum cost design of PC I-girder bridge system. It is difficult to solve the proposed constrained global optimization problems of 13 numbers of mixed integers, discrete and continuous design variable and a large number of implicit constraints by using gradient based optimization methods. It has been shown that such a problem can, however, be easily solved using EVOP with a relatively small number of function evaluations. To demonstrate that optimization of such problems really results in considerable economy, a practical example of this application is presented here and it results in an optimum solution or the minimum cost design which leads to a saving of around 36%. Furthermore, the computer time used for the design was merely a total of 10 s. So far we have discussed about the optimization of the bridges considering only the construction cost. In reality, service life costs (inspection, maintenance and rehabilitation) may also be significant in comparison to initial construction cost of a bridge project. Furthermore, consideration of the uncertainties related to materials, loads and environment may alter the optimum design [35]. So, further research is necessary to extend the proposed study considering the service life costs, all the uncertainties related to materials and structures. For this purpose, multi-objective optimization approaches should further be explored to consider both costs and structural robustness.

Appendix A

See Table A1.

$$V_{GC} = [100X_3 + 5000 + f(X_6)\{X_2 - 100 - 1.125X_5 + 0.125f(X_6) - 0.125X_4\} + 1.125X_4X_5 - 0.25\pi X_7\{f(X_6) - 80\}^2]L \quad (A1)$$

$$V_{DC} = X_1X_{11}L \quad (A2)$$

$$W_{PS} = 140\gamma_{st}X_6X_7L \quad (A3)$$

$$W_{OSD}\{2X_{12}(X_{11} - 57)X_1L + g(x)X_1L + 0.265X_1L\}\gamma_{st} \quad (A4)$$

where γ_{st} = unit weight of prestressing steel.
and $g(x) = \min(0.007216/\sqrt{X_1 - 0.5X_3}, 0.67) \times X_{12} * (X_{11} - 57)$

$$W_{OSG} = A_VL_V\gamma_{st} \quad (A5)$$

where L_V is implicitly related to many of the design variables.

$$W_{OSN} = 0.25[X_{13}X_4(X_2 + 0.5X_{11}) - \{0.265 + g(x)\}X_1]L\gamma_{st} \quad (A6)$$

References

[1] Thierauf G, Cai JB. Parallel evolution strategy for solving structural optimization. Eng Struct 1997;19(4):318–24.
[2] Nikolaos DL, Manolis P, George K. Structural optimization using evolutionary algorithms. Comput Struct 2002;80:571–89.

[3] Toğan V, Daloğlu A. Optimization of 3d trusses with adaptive approach in genetic algorithms. Eng Struct 2006;28:1019–27.
[4] Kwak HG, Noh SH. Determination of strut-and-tie models using evolutionary structural optimization. Eng Struct 2006;28:1440–9.
[5] Dimopoulos GG. Mixed-variable engineering optimization based on evolutionary and social metaphors. Comput Methods Appl Mech Eng 2007;196(4–6):803–17.
[6] Kalanta S, Atkočiūnas J, Venskus A. Discrete optimization problems of the steel bar structures. Eng Struct 2009;31:1298–304.
[7] Barakat SA, Altoubat S. Application of evolutionary global optimization techniques in the design of RC water tanks. Eng Struct 2009;31:332–44.
[8] Parsopoulos KE, Vrahatis MN. Recent approaches to global optimization problems through particle swarm optimization. Nat Comput 2002;1:235–306.
[9] Li LJ, Huang ZB, Liu F. A heuristic particle swarm optimization method for truss structures with discrete variables. Comput Struct 2009;87:435–44.
[10] Kaveh A, Talatahari S. An improved ant colony optimization of planar steel frames. Eng Struct 2010;32:864–73.
[11] Torn A, Zilinskas A. Global optimization. Gn – Griewank [Griewank 1981], (N = 10). vol. 350. Springer-Verlag; 1987. p. 186. ISBN: 3-540-50871-6, 0-387-50871-6.
[12] Ghani SN. A versatile algorithm for optimization of a nonlinear nondifferentiable constrained objective function. UKAEA Harwell report number R13714. HMSO Publications Centre, PO Box 276, London SW85DT; 1989. ISBN: 0-7058-1566-8.
[13] Ghani SN. Performance of global optimisation algorithm EVOP for non-linear non-differentiable constrained objective functions. In: Proceedings of the IEEE international conference on evolutionary computation (IEEE ICEC'95), vol. 1, The University of Western Australia, Perth, Western Australia; 1995. p. 320–5.
[14] Ghani SN. EVOP manual; 2008. p. 25 and 122. <http://www.OptimumSystemDesigners.com> [17.12.08].
[15] Adeli H, Sarma KC. Cost optimization of structures. England: John Wiley & Sons Ltd.; 2006.
[16] Hassanain MA, Loov RE. Cost optimization of concrete bridge infrastructure. Can J Civ Eng 2003;30:841–9.
[17] Torres GGB, Brotchie JF, Cornell CA. A program for the optimum design of prestressed concrete highway bridges. PCI J 1966;11(3):63–71.
[18] Fereig SM. Preliminary design of standard CPCI prestressed bridge girders by linear programming. Can J Civ Eng 1985;12:213–25.
[19] Fereig SM. An application of linear programming to bridge design with standard prestressed girders. Comput Struct 1994;50(4):455–69.
[20] Fereig SM. Economic preliminary design of bridges with prestressed I-girders. J Bridge Eng ASCE 1996;1(1):18–25.
[21] Kirsch U. A bounding procedure for synthesis of prestressed systems. Comput Struct 1985;20(5):885–95.
[22] Cohn MZ, MacRae AJ. Optimization of structural concrete beams. J Struct Eng ASCE 1984;110(7):1573–88.
[23] Cohn MZ, MacRae AJ. Prestressing optimization and its implications for design. PCI J 1984;29(4):68–83.
[24] Lounis Z, Cohn MZ. Optimization of precast prestressed concrete bridge girder systems. PCI J 1993;38(4):60–78.
[25] Sirca GF, Adeli H. Cost optimization of prestressed concrete bridges. J Struct Eng ASCE 2005;131(3):380–8.
[26] Kirsch U. Two-level optimization of prestressed structures. Eng Struct 1997;19(4):309–17.
[27] Ayvaz Y, Aydin Z. Optimum topology and shape design of prestressed concrete bridge girders using a genetic algorithm. Struct Multidisc Optim Ind Appl 2009. http://dx.doi.org/10.1007/s00158-009-0404-.
[28] Ahsan R, Rana S, Ghani SN. Cost optimum design of post-tensioned I-girder bridge using global optimization algorithm. J Struct Eng ASCE 2012;138(2):273–84.
[29] American Association of State Highway and Transportation Officials (AASHTO). Standard specifications for highway bridges. 17th ed. Washington, DC; 2002.
[30] Highway structures design handbook. vols. I and II. Pittsburgh: AISC Marketing, Inc.; 1986.
[31] Precast/Prestressed Concrete Institute (PCI). PCI bridge design manual. Chicago, IL; 2003.
[32] Roads and Highway Department (RHD). Schedule of rates. Dhaka, Bangladesh; 2006.
[33] Freyssinet Inc. The C range post-tensioning system; 1999. <http://www.freyssinet.com> [10.05.10].
[34] Bureau of Research Testing & Consultation (BRTC). Teesta Bridge project report. File no. 1247. Dept. of Civil Engineering Library, Bangladesh University of Engineering and Technology, Dhaka, Bangladesh; 2007.
[35] Okasha NM, Frangopol DM. Lifetime-oriented multi-objective optimization of structural maintenance considering system reliability, redundancy and life-cycle cost using GA. Struct Saf 2009;31(6):460–74.